J Bio Tribo Corros (2017) 3:7
DOI 10.1007/s40735-016-0066-8

Mechanistic Study of the Wear of Ceramic Heads by Metallic Stems in Modular Implants

S. J. Bull[1] · N. Moharrami[1] · D. Langton[1]

Received: 15 September 2016 / Revised: 4 November 2016 / Accepted: 20 November 2016 / Published online: 2 December 2016

Abstract Titanium-based and cobalt–chrome alloys as well as some ceramics have been widely used in orthopaedic applications as these materials can significantly enhance the quality of human life as implant materials. However, the in vivo performance of some large-diameter metal-on-metal joints is unsatisfactory, and concerns have been expressed over the wear behaviour of the materials and released metal ions affecting local tissue and more distant organs. The longevity of these materials is highly influenced by their mechanical properties and this has driven the development of alternative ceramic components with greatly improved tribological performance. Even these novel materials are not immune to damage, for instance in some devices alumina-based ceramic components articulate with titanium alloy counterfaces (e.g. in the taper connections of titanium alloy stems and zirconia-toughened alumina femoral heads in modern modular designs) and damage has been reported of the harder ceramic surface by the softer titanium alloy component. In such contacts, the chemically inert ceramic component is not expected to corrode, so the electrochemical damage mechanisms often suggested for metal–metal contacts are not appropriate. This study attempts to understand why this wear might occur by investigating bulk and surface mechanical properties (such as hardness and Young's modulus) of a number of hip implants and test samples using a Hysitron Triboindenter. AFM images were also obtained to determine the contact area and hence, pile-up correction factors for the metallic material. It was found that the alumina ceramic heads were generally subject to chemomechanical softening after exposure to water for an extended period whilst titanium alloy oxidised preferentially generating a hard oxide surface which was not softened by water. Furthermore, the oxidised titanium showed significantly higher hardness values therefore damaging the chemomechanically softened alumina material.

Keywords Nanoindentation · Titanium alloy · Zirconia toughened alumina · Orthopaedic implant

1 Introduction

In recent orthopaedic practice, total hip replacements are one of the most common successfully performed and cost-effective procedures. The human body with its highly corrosive environment requires a material with good resistance to corrosion, an excellent biocompatibility with its surrounding environment and adequate mechanical strength and stiffness to give a long life component.

The main purpose of the replacement of any hip joint is to implant a prosthesis which reduces pain, allows mobility and has sufficient longevity to last for the life of the patient. Since 1960 when the very first successful total hip replacement was designed [1], there have been several improvements in materials selection and the design of the implants to increase their life. In fact, due to the changes in lifestyle, there is a growing demand for hip replacement in younger patients. Therefore, it is necessary to improve the average life of the implants from ~10 to 30 years [2]. To achieve this different bearing surface combinations for the implant have been developed since wear debris from the articulating surfaces can lead to joint loosening and the need for revision. Such combinations include metal-on-

✉ S. J. Bull
steve.bull@ncl.ac.uk

[1] Chemical Engineering and Advanced Materials, Newcastle University, Newcastle upon Tyne NE1 7RU, UK

metal (MoM), metal-on-plastic (UHMWPE), ceramic-on-ceramic (CoC) and ceramic-on-plastic (UHMWPE) [3]. Metal-on-plastic systems have been found to generate significant plastic wear debris leading to problems with joint loosening, and this has driven a change to MoM systems. However, there are concerns about the MoM systems, particularly when the femoral head is large, and higher than expected revision rates are observed which has made the use of ceramic components more attractive. When comparing the ceramic femoral head systems to other types of available implants, the ceramics show less wear [4] and therefore less loosening of the implant. Problems with fracture of the ceramics have been addressed by improvements in manufacture and the use of toughened ceramic materials [4].

Titanium and its alloys have been successfully used in the human body as implant materials due to their high biocompatibility, corrosion resistance and hardness [5–7]. Moreover, when comparing other orthopaedic metals such as stainless steel and cobalt chromium alloys, titanium with its lighter weight [8], lower elastic modulus and higher strength-to-weight ratio [9] is a more suitable material for various orthopaedic applications.

To make best use of these material combinations, the original fixed-head femoral prostheses (a single piece design) has been replaced by a modular design (interchangeable parts) with a detachable femoral head and stem [10, 11]. Human bone with elastic modulus <40 GPa [12] requires a material with low elastic modulus to reduce stress shielding of the femur. Therefore, to reduce the strain between the bone and implant interface, the stem portion of the total joint replacements is usually built with a titanium alloy (Ti6Al4V) which has a lower elastic modulus compared to the cobalt chromium alloys or stainless steels used in orthopaedic implants. In some low stress applications (e.g. dental), commercially pure titanium (cp-Ti) has been used, but this has lower strength than the alloy used in orthopaedic applications despite a similar stiffness. Both cp-Ti and Ti6Al4V form a passive titanium oxide in service which protects the material from corrosion and have very similar osseointegration performance.

As the human body is highly corrosive environment [13], the biocompatibility and corrosion resistance of each individual component in addition to their mechanical properties play a significant role in the longevity of the joint replacement [14]. The high hardness value of the ceramic components and a very smooth surface finish are major reasons for better wear resistance. Therefore, with low levels of wear, ceramics can be reliable materials to replace metal alloys used in MoM hip joints. Cobalt–chrome or ceramics are thus used for the femoral head because of their higher hardness and superior wear resistance. In addition, the release of metal ions into the body by tribocorrosion processes can be significant in some metal alloy systems with potentially deleterious effects (e.g. the release of cobalt ions from cobalt–chrome) and this suggests that inert ceramic materials where corrosion is minimal might be the better choice for articulating orthopaedic components.

Despite its lower hardness, it has been reported in the literature [10, 15] that titanium can abrasively damage a cobalt chromium femoral head in the taper connection. When two different metals are joined in the human body (a corrosive environment), there are several contributions to this failure. Corrosion of the alloys [16], electrochemical effects due to interaction with surroundings [14] and wear [17] are the three major causes which require study for understanding of the failure process. As was shown previously, [18] titanium becomes oxidised when used in vivo and a thick oxide layer built on the surface makes it harder than cobalt–chrome which is only covered with a very thin oxide. Consequently, the harder titanium oxide layer on the surface of the stem can easily wear away the cobalt–chrome femoral head in the connection between the neck of the stem and the head. For such metallic systems effects of the environment on wear in realistic operating conditions are well studied [e.g. 19–21]. However, much less is known about the failure of the ceramic heads. Considering the superior corrosion resistance of ZTA, corrosion and the electrochemical effects of the surrounding environment should not be significant and yet such damage has been observed within the taper of a ceramic head on a titanium alloy stem. In this study, we focus on understanding the failure of ceramic hip replacements due to wear by softer titanium stem.

2 Experimental

2.1 Materials and Characterisation

The mechanical properties of titanium-based alloy stem (Ti–6Al–4V) and zirconia-toughened alumina (ZTA) ceramic femoral heads used in total hip replacements have been investigated. Commercial modular implants were used with the as-received surface finish. The composition and structure of the samples were confirmed by energy dispersive X-ray analysis (EDX) in the scanning electron microscope (SEM), X-ray diffraction (XRD) and Raman spectroscopy. These techniques were also used to look for the existence of surface reaction layers.

2.2 Methodology

Surface properties like hardness of materials can be changed based on the environment in which the components

operate in; for instance the titanium components are expected to be oxidised in the body and the ceramic components may be chemomechanically softened [22]. The key intention of this work was to investigate the changes in the surface mechanical properties of the materials used after exposure to an inert environment and one that is representative of exposure in the human body. Initially, to compare the hardness and modulus values, nanoindentation tests were carried out using as-received samples. Next, both the ceramic and the metal alloy samples were placed in ethanol for a period of three weeks to gradually dry their surface. After evaporating any remaining liquid from the sample surface with a warm, dry air flow, nanoindentation tests were carried out under the same indentation test conditions. Finally, the samples were treated chemically to obtain the mechanical properties using conditions that are representative of the actual body environment and thereby increasing the relevance of the results. This was performed by placing them in a 500 mL solution of distilled water containing 175.32 g/l (3 M) of NaCl at 37 °C for a period of three weeks.

2.3 Nanoindentation Testing

In this work, a Hysitron Triboindenter was used to measure the mechanical behaviour of the materials under investigation. The tests were carried out using a Berkovich indenter tip with an effective tip radius of 200 nm. Atomic force microscopy (AFM) images were captured using the same indenter probe before and after each indentation. These images can be used to map the surface of the materials before indentation to understand where the indentation takes place in addition to understanding, for example, the effects of surface roughness on the data obtained. Mapping the surface of the samples by AFM after indentation tests can be used to measure the true contact area in case of appearance of pile-up or sink-in [23]. Prior to the nanoindentation tests, the Oliver and Pharr method [24] was used to calibrate both the instrument stiffness and the tip-end shape. Aluminium and fused silica certified reference samples were used for the calibration. Samples were placed for 24 h in the nanoindentation chamber prior to any indentation test to reduce the influence of the temperature differences between the sample and the indenter tip. Indentation tests were carried out using two types of test protocol, displacement control and open loop mode, using a single loading and unloading cycle. At the end of the loading cycle, to minimise the effect of creep on the results a 4 s hold was used at the maximum load. An array of one hundred indentations with 20 μm spacing was used in each test at peak loads between 100 μN and 3 mN corresponding to displacements in the range 15–150 nm at loading/unloading rates of 1 mN/s. Some initial experiments on ZTA and tests on titanium alloy samples were carried out under displacement control at 10 nm/s to determine if there was any time-dependent deformation; however, this was not significant for the ZTA.

3 Results and Discussion

X-ray diffraction studies (Fig. 1) and EDX analysis (Table 1) of the titanium stem and ZTA femoral head show that these are the expected materials in the as-received state. For the titanium alloy, the XRD pattern showed the normal α/β titanium structure of Ti6Al4V and the EDX data clearly showed the Al and V content. There are no signs of a discrete oxide layer on the surface of the as-received Ti6Al4V. The titanium oxide that forms on this alloy in vivo has been previously shown to be amorphous in transmission electron microscopy studies [25], and this was confirmed in this study. The ZTA XRD pattern was very well fitted by tetragonal (as opposed to cubic) zirconia and α-Al_2O_3, and the zirconia was partially stabilised by yttria. There were no obvious peaks from yttrium in the EDX spectra but the aluminium to zirconium ratio is

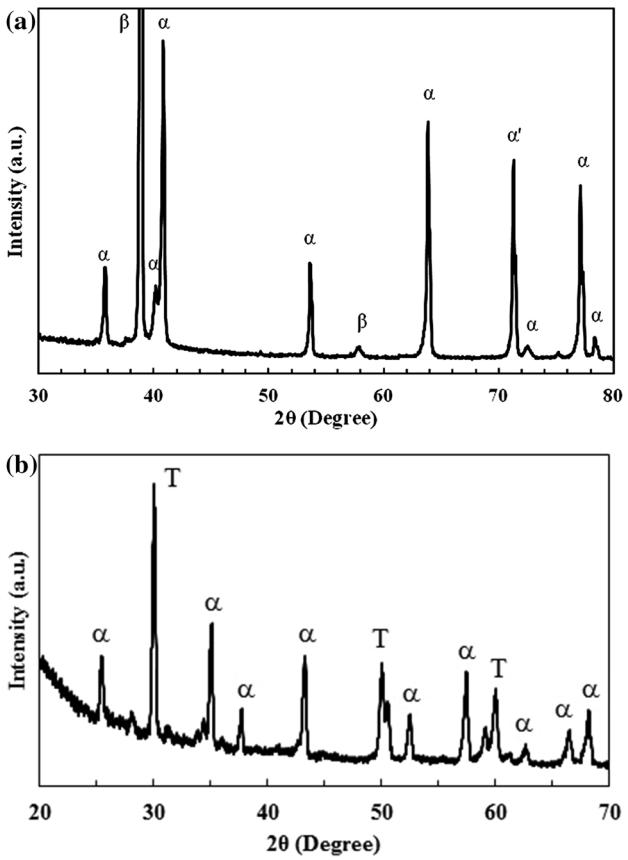

Fig. 1 X-ray diffraction patterns for **a** the titanium stem and **b** the ZTA femoral head

Table 1 EDX results for the ZTA ceramic and Ti–6Al–4V samples before and after exposure to salt water

Sample	Element	As-received (at.%)	After salt water (at.%)
ZTA	Al	23.9 ± 0.7	23.6 ± 0.8
	Zr	3.8 ± 0.5	3.9 ± 0.4
	O	58.4 ± 0.9	58.1 ± 0.9
	C	13.9 ± 0.6	14.0 ± 0.6
Ti–6Al–4V	Ti	89.7 ± 0.9	61.2 ± 0.9
	Al	6.7 ± 0.7	5.3 ± 0.5
	V	3.6 ± 0.5	0.1 ± 0.5
	O	0 ± 0.5	23.6 ± 0.7
	C	0 ± 0.5	9.8 ± 0.5

consistent with the alumina with 17.5 vol% YSZ (8% yttria) which is used in femoral heads. In such circumstances, the yttrium peaks are below the detection limit of EDX in the system used.

After exposure to salt water, there is no change in the XRD patterns for each material but there is considerable evidence for oxidation of the titanium alloy surface in the EDX data (Table 1). It should be noted that the presence of large amounts of carbon in the ZTA and exposed titanium samples is due to the deposition of a very thin layer of carbon on the sample surface prior to EDX analysis; carbon coating is normally used to improve secondary electron emission, increasing the electrical conductivity and reducing sample charging for SEM and EDX analysis.

To evaluate the damage resistance of the surface, the hardness of the ceramic and titanium samples were tested using the nanoindentation technique. The first set of nanoindentation data shown in Fig. 2 was collected from the as-received ZTA ceramic sample. These tests were performed under displacement control. For the first 60 nm contact depth, both the hardness and Young's modulus values decrease slightly, whilst the contact depth is increasing. However, at contact depths higher than this, the values remain constant. This is the normal indentation size effect behaviour expected in crystalline ceramic materials [e.g. 26, 27]. In fact metals, ceramics and polymers show this effect with hardness increasing as the contact size decreases, but the extent to which it is observed varies with the effect being most pronounced for ceramic materials due to their high hardness and stiffness. The indentation size effect in ceramics also depends on the sharpness of the indenter with blunt diamonds generating higher hardness at low penetration depths when compared to sharp indenters. In this study, a relatively sharp Berkovich indenter with a tip-end radius of 200 nm was used to reduce the observed indentation size effect but even the sharpest tips available (with a 50 nm end radius) would show the effect but shifted to lower indentation depths; the plateau in hardness

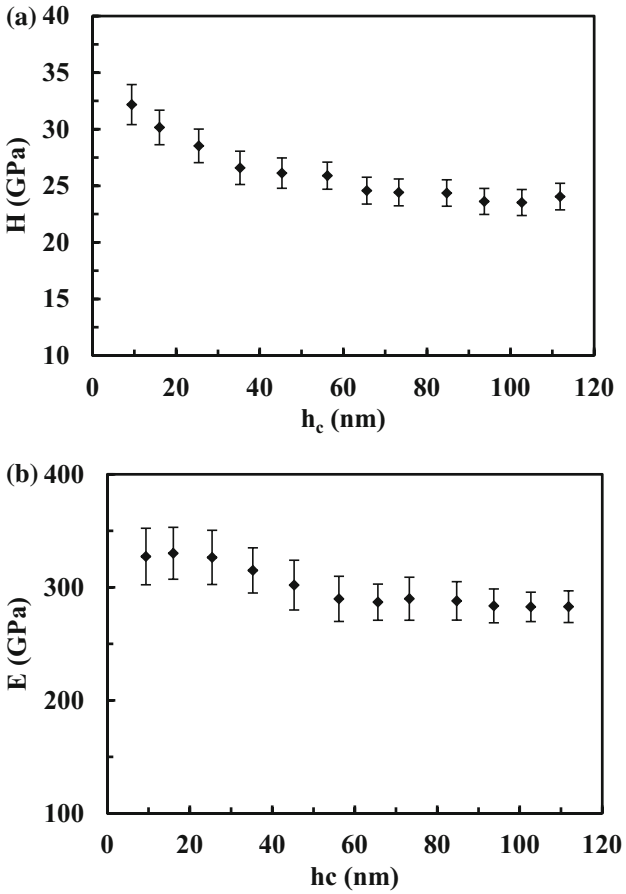

Fig. 2 **a** Hardness and **b** Young's modulus of the ZTA ceramic

would occur at lower contact depth than the 60 nm observed here. For this reason, it is difficult to make comparisons between tests made with different indenters, and it is necessary to check that the tip geometry and end radius did not change appreciably during the tests carried out. The Berkovich tip-end shape used here was calibrated by measurements on a fused silica standard before and after testing the ceramic samples, and no appreciable change was observed so the comparisons between different test conditions are meaningful.

The average hardness for the contact depths <50 nm is 28 ± 2 GPa, and for higher contact depths the average value drops to 24 ± 0.5 GPa. Similar to hardness values, the average modulus drops from 315 ± 16 to 285 ± 3 GPa for the contact depths <50 nm and higher contact depths, respectively. These values are comparable to the results of bulk tests on similar material (9.8 N Vickers hardness 15 GPa, Young's Modulus from 3 point bending 300 GPa), but the nanoindentation hardness is somewhat higher.

The reason for the high hardness can be seen when the heterogeneous nature of the microstructure is taken into consideration. Backscattered electron images of the ZTA surface taken in the SEM show that the material consists of

α-alumina grains with separate smaller YSZ grains at their boundaries (Fig. 3). The alumina grain size is 500–600 nm, whilst the YSZ grain size is close to 300 nm. When nanoindentation tests are made with a maximum displacement of 150 nm (in the plateau region in Fig. 1a) using the hardness and Modulus values determined in the test, the plastic zone radius is 530 nm according to the equation of Chen and Bull [28]:

$$R_p = (4.5451 - 12.07H/E)\delta_{max} \quad (1)$$

Thus, the plastic deformation can be constrained within a single alumina grain; if this occurs, the hardness recovered is that of alumina (~25 GPa in nanoindentation tests [18, 29]). Using the properties of YSZ measured by nanoindentation [30], the plastic zone radius is 570 nm by the same approach. The plastic deformation therefore encompasses several grains, and the hardness will be critically dependent on the location where the measurement is made, but it will be close to the bulk alumina test values.

There is less point to point variation in the elastic properties of the samples since Young's Modulus obtained by indentation is a long range property and is averaged over a much larger volume of the sample.

In comparison to the values obtained for titanium alloy reported previously [18], the hardness and modulus are both higher for the ZTA sample tested here. Titanium with average hardness of 5.4 GPa for the low contact depths (<80 nm) is very much softer than ZTA ceramic closer to the surface. However, in the same work, it was suggested that when titanium is used in the human body, due to surface oxidation, its hardness increases from 5.4 to 12 GPa and continues increasing to 16 GPa for higher contact depths. Thus, it is unlikely to be able to damage the ZTA as the titanium oxide is softer across the entire contact depth range. Therefore, some further change to the surfaces must have occurred for abrasive damage to be manifested—this is likely to have come from other interactions with the environment around the ceramic.

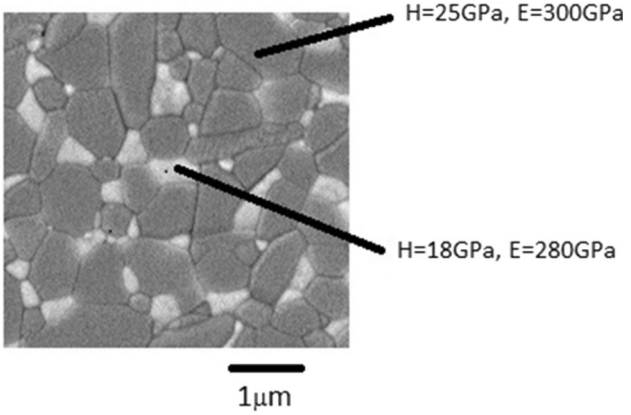

Fig. 3 SEM backscattered electron image of ZTA. The *light regions* are yttria-stabilised zirconia grains and the *darker regions* are α-alumina. The heterogeneous nature of the microstructure leads to variations in the properties measured by nanoindentation

To investigate possible effects of the environment on the mechanical properties of ZTA ceramic femoral heads, samples were treated under two different conditions for comparison. Initially, samples were left in ethanol for a period of three weeks to remove any existing water from the surface. Afterwards, nanoindentation tests were carried out immediately on the dried surface of the ceramic samples. A large indent was placed at the crown of the head to locate the position of the test array accurately. It should be noted that in order to keep the natural humidity of the test atmosphere as low as possible, the tested samples were surrounded by silica gel inside the sealed nanoindentation chamber. After the first sets of data were collected, the samples were placed in salt water at a fixed temperature of 37 °C for three weeks. The nanoindentation tests were then repeated after drying. The large indent was located by the Nanoindenter optics and used to position the indentation array at 10 microns offset from the first set of measurements. In this way, the same region of the sample is tested and the effects of material heterogeneity are reduced.

The nanoindentation data are compared in Fig. 4 for both dried and wet samples obtained using the open loop mode test protocol—this was used as time-dependent deformation (creep) was not expected to affect the results. There are significant differences between the data obtained from dried and wet ZTA samples for the contact depths <60 nm. The average nanoindentation hardness for the samples dried using ethanol for low contact depths is 37 ± 3 GPa and drops dramatically to 19 ± 3 GPa for after the samples were exposed to water. This is similar to the modulus which decreases from 407 ± 39 GPa for dried sample to 267 ± 12 GPa for wet sample. For the contact depths more than 60 nm, both the hardness and modulus data exhibit similar values within a reasonable error margin for the nanoindentation test. When the results from Fig. 2 are compared to that of Fig. 4, the average hardness and modulus are different for all three conditions mainly near the surface for the depths <50 nm. It is clear that the data in Fig. 2 come from alumina-rich materials, whilst the data in Fig. 4 come from zirconia-rich regions and the heterogeneity of the sample makes comparisons difficult unless the same general region of the sample is tested.

For comparison, similar tests were carried out on the Ti–6Al–4V stem under the same conditions. First sets of data were collected for the as-received sample. Next, the sample was kept in ethanol for three weeks, and further nanoindentation tests were applied on the dried surface of the titanium alloy. Finally, the sample was treated in salt water for three weeks and more indentation tests were performed. It should be noted that all the indentation conditions such

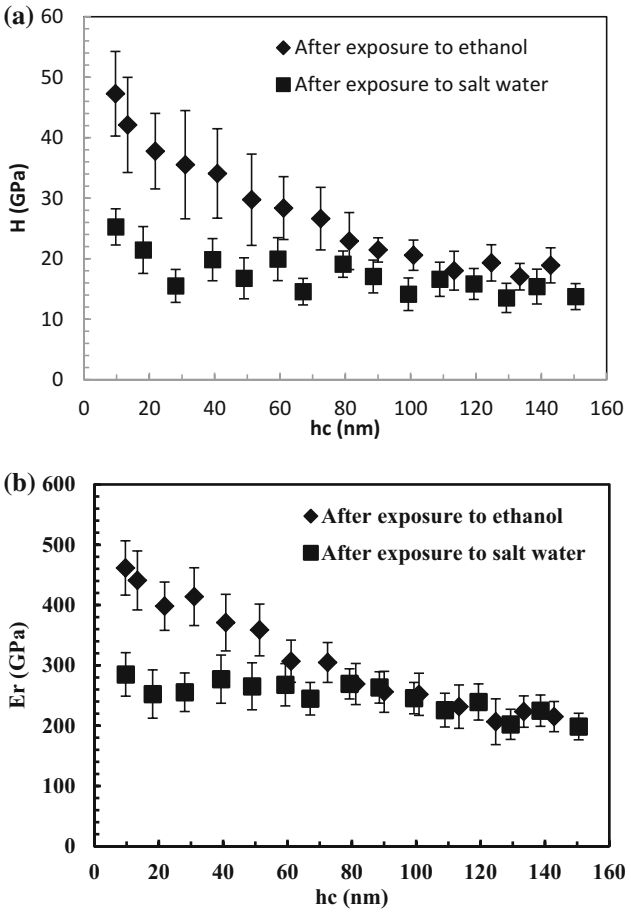

Fig. 4 **a** Hardness and **b** elastic modulus of the ZTA ceramic femoral head after exposure to ethanol and water

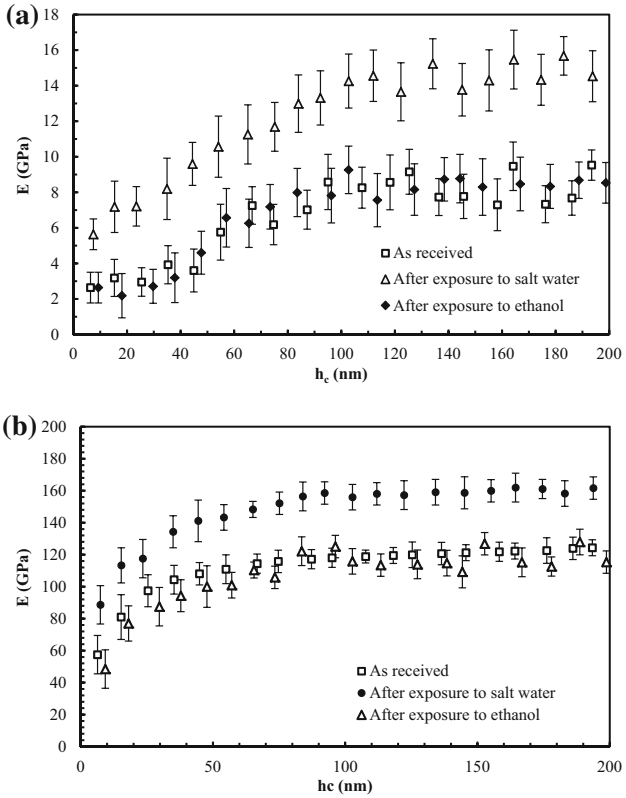

Fig. 5 Comparison of **a** hardness and **b** elastic modulus for Ti–6Al–4V for all three types of exposure conditions

as load function and test protocols were kept the same for both titanium alloys and ceramic heads. The average hardness and modulus data obtained from titanium alloy under three different conditions after pile-up correction are shown in Fig. 5 for comparison. Unlike the ZTA case, the hardness increases with contact depth and does not show conventional indentation size effect behaviour which occurs at higher penetration depths. This behaviour is attributed to the transition from elastic to elastic–plastic behaviour and work hardening effects in the metal [27], but this may also be influenced by the presence of a porous external oxide layer. At contact depths <100 nm, the validity of the Oliver and Pharr method [24] for extracting hardness and modulus data from the measured nanoindentation response is questionable.

The hardness and modulus data measured by the method of Oliver and Pharr [24] for titanium alloys were improved by calculating the true contact area using the AFM images. One of the potential issues using the Oliver and Pharr method to measure the hardness and elastic modulus is pile-up. For highly elastic materials such as glass and ceramic, during the indentation test, materials tend to sink-in near the edges of the indenter probe. However, for softer, more plastic materials, for instance soft metals, material tends to pile-up around the indenter edges. Therefore, pile-up around the indentation area leads to a significant increase in the contact area which can support some of the applied load and therefore influence the measured data. Figure 6 shows examples of AFM images obtained before and after nanoindentation. The appearance of the pile-up around the indenter can be seen clearly, and the AFM data was used to estimate the true contact area and correct the hardness and modulus data for the effects of pile-up.

When the results for the titanium alloy shown in Fig. 5 are compared, there are great variations between the data obtained from the sample kept in salt water to the other two

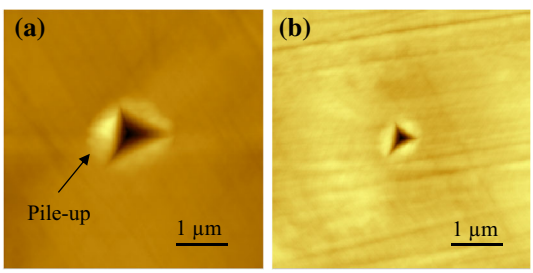

Fig. 6 AFM images of titanium alloy under **a** 5 mN and **b** 2 mN peak loads during nanoindentation

environments. As mentioned earlier, titanium gets oxidised when exposed to salt water or in vivo, and therefore its surface mechanical properties are modified. From the values shown in Fig. 5, it is clear that because of the oxidation, the hardness and modulus increase. However, there are no significant differences between the hardness and elastic modulus of the sample kept in ethanol and the as-received sample. To better understand and also compare all, the hardness and modulus data obtained for titanium and ZTA ceramic are summarised in Table 2.

When the results for titanium alloys and ZTA ceramics are compared, the immersion of the ceramic in water leads to a considerable softening—this is termed a chemomechanical effect. Zirconium and aluminium oxide show softening whereas titanium oxide does not under the same conditions—hence the titanium is able to scratch the ceramic surface. It has been shown that titanium becomes harder when used in vivo [18] and this is due to the spontaneous build-up of a stable and inert oxide layer [31, 32]. This oxide is substantially amorphous [25] and is therefore not as likely to show significant chemomechanical effects [22].

The change in the mechanical properties can be attributed to complex interplay of physisorption as well as chemical reactions occurring on the surface of the samples. Previously, the chemomechanical softening effect on the surface layer was attributed to a weak hydroxide layer produced on the surface [22]. However, there is no experimental evidence confirming the creation of the hydroxide layer on the surface in this study; XRD and Raman spectroscopy were used here to determine the structure of the ceramic head and to look for the existence of surface reaction layers. Figure 7 shows the Raman spectrum for the ZTA ceramic head before and after being placed in salt water for three weeks. There was no difference between the spectra, and no obvious surface reaction layers were found by any technique used in this study.

If the hydroxide layer is not formed, a second mechanism is most likely since this is known to occur in crystalline alumina [22]. The adsorbed water (OH on the surface) modifies the surface charge and the local electronic structure in the surface region and subsequently

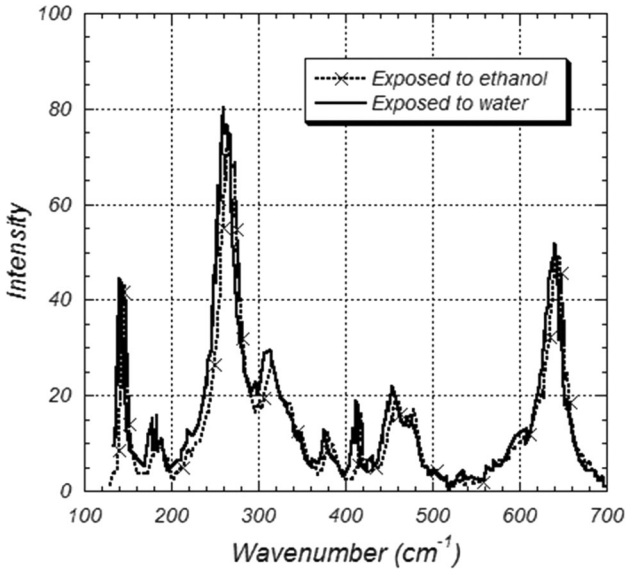

Fig. 7 Raman spectra of ZTA after exposure to ethanol and water. There are no significant differences in the two environments

increases the mobility of dislocations which are the carriers of plastic deformation in crystalline materials. Dislocations in ionic materials are charged, so it is not surprising that modifying the surface charge state will affect their mobility. The result is a water-softened surface layer with lower hardness. In sapphire, the water-softened layer is around 5 nm thick and therefore it is only the low load nanoindentation data which is affected [22]. When testing at low loads, the data produced reflect the transition from elastic to plastic behaviour and any chemomechanical effects—in such circumstances the hardness is low for crystalline ceramics.

Thus, the surface hardness of the crystalline ZTA is reduced by exposure to water over a depth of a few nanometres. Similarly, the surface hardness of the titanium alloy is increased over a similar depth due to the formation of an amorphous oxide which is not chemomechanically softened. It is this that leads to the observed damage if the oxidised titanium slides over the chemomechanically softened alumina.

Table 2 Hardness and modulus results obtained from ZTA ceramic and Ti–6Al–4V samples under three different conditions

Sample	Conditions	E (GPa)		H (GPa)	
		hc < 60 nm	hc > 60 nm	hc < 60 nm	hc > 60 nm
ZTA	As-received	315 ± 16	285 ± 3	28 ± 2	24 ± 0.5
	Exposure to ethanol	407 ± 39	251 ± 25	37 ± 3	21 ± 3
	Exposure to water	267 ± 12	234 ± 14	19 ± 3	15 ± 1
Ti–6Al–4V	As-received	99 ± 18	121 ± 2	3 ± 1	8 ± 1
	Exposure to ethanol	90 ± 13	118 ± 6	3 ± 1	8 ± 1
	Exposure to water	129 ± 12	158 ± 2	9 ± 1	15 ± 1

4 Conclusions

Unexpected wear of the ZTA ceramic femoral heads used in total hip replacement by titanium alloy stems in the taper connection has been investigated. The results show that when materials are used in human body, their surface mechanical properties can be changed significantly. In vivo oxidation of the titanium alloy causes the stem to become harder and the ceramic component becomes softer due to chemomechanical effects on the surface. Therefore, harder oxidised titanium can wear the softened ceramic femoral head in the taper connection in the studied conditions.

Acknowledgements This work was funded by the Newcastle University.

Compliance with Ethical Standards

Conflict of interest There are no conflicts of interest arising from the involvement of other parties either internal or external to the University.

References

1. Gomez PF, Morcuende JA (2005) A historical and economic perspective on Sir John Charnley, Chas F. Thackray Limited, and the early arthroplasty industry. Iowa Orthop J 25:30–37
2. De Aza AH, Chevalier J, Fantozzi G, Schehl M, Torrecillas R (2002) Crack growth resistance of alumina, zirconia and zirconia toughened alumina ceramics for joint prostheses. Biomaterials 23:937–945
3. Di Puccio F, Mattei L (2015) Biotribology of artificial hip joints. World J Orthop 6:77–94
4. Dorlot JM, Christel P, Meunier A (1989) Wear analysis of retrieved alumina heads and sockets of hip prostheses. J Biomed Mater Res Appl Biomater 23:299–310
5. Punt I, Visser V, Rhijn L, Kurtz S, Antonis J, Schurink G, Ooij A (2008) Complications and reoperations of the SB Charite lumbar disc prosthesis: experience in 75 patients. Eur Spine J 17:36–43
6. Takeuchi M, Abe Y, Yoshida Y, Nakayama Y, Okazaki M, Akagawa Y (2003) Acid pretreatment of titanium implants. Biomaterials 24:1821–1827
7. Zhou Y-L, Niinomi M, Akahori T, Nakai M, Fukui H (2007) Comparison of various properties between titanium-tantalum alloy and pure titanium for biomedical applications. Mater Trans 48:380–384
8. Imam MA, Fraker AC (1996) Titanium alloys as implant materials. In: Proceedings of the 1994 symposium on medical applications of titanium and its alloys: the material and biological issues, ASTM, Phoenix, AZ, 15–16 Nov 1994, p 3
9. Bischoff UW, Freeman MAR, Smith D, Tuke MA, Gregson PJ (1994) Wear induced by motion between bone and titanium or cobalt-chrome alloys. J Bone Jt Surg 76B:713–716
10. Collier JP, Surprenant VA, Jensen RE, Mayor MB, Surprenant HP (1992) Corrosion between the components of modular femoral hip prostheses. J Bone Jt Surg 74:511–517
11. Cohen D (2012) How safe are metal-on-metal hip implants? Br Med J 344:e1410
12. Long M, Rack HJ (1998) Titanium alloys in total joint replacement—a materials science perspective. Biomaterials 19:1621–1716
13. Navarro M, Michiardi A, Castano O, Planell JA (2008) Biomaterials in orthopaedics. J R Soc Interface 5:1137–1158
14. Hansen DC (2008) Metal corrosion in the human body: the ultimate bio-corrosion scenario. Electrochem Soc Interface 17:31–34
15. Panagiotidou A, Meswania J, Hua J, Muirhead-Allwood S, Hart A, Blunn G (2013) Enhanced wear and corrosion in modular tapers in total hip replacement is associated with the contact area and surface topography. J Orthop Res 31:2032–2039
16. Metikos-Hukovic M, Babic R (2007) Passivation and corrosion behaviours of cobalt and cobalt-chromium-molybdenum alloy. Corros Sci 49:3570–3579
17. Shahgaldi BF, Heatley FW, Dewar A, Corrin B (1995) In-vivo corrosion of cobalt-chromium and titanium wear particles. J Bone Joint Surg 77B:962–966
18. Moharrami N, Langton DJ, Sayginer O, Bull SJ (2013) Why does titanium alloy wear cobalt chrome alloy despite lower bulk hardness: a nanoindentation study? Thin Solid Films 549:79–86
19. Fischer TE (1988) Tribochemistry. Annu Rev Mater Sci 18:303–323
20. Czernuszka JT, Page TF (1985) The importance of microscopy in studying the wear behaviour of ceramics. J Microsc 140:159–169
21. Sugita T, Ueda K, Kanemura Y (1984) Material removal mechanism of silicon-nitride during rubbing in water. Wear 97:1–8
22. Bull SJ, Moharrami N, Hainsworth SV, Page TF (2016) The origins of chemomechanical effects in the low-load indentation hardness and tribology of ceramic materials. J Mater Sci 51:107–125
23. Moharrami N, Bull SJ (2014) A comparison of nanoindentation pile-up in bulk materials and thin films. Thin Solid Films 572:189–199
24. Oliver WC, Pharr GM (1992) An improved technique for determining hardness and elastic modulus using load and displacement sensing indentation experiments. J Mater Res 7:1564–1583
25. Palmqvist A, Lindberg F, Emanuelsson L, Branemark R, Engqvist H, Thomsen P (2010) Morphological studies on machined implants of commercially pure titanium and titanium alloy (Ti6Al4V) in the rabbit. J Biomed Mater Res A92: 1476–1486
26. Bull SJ, Page TF, Yoffe EH (1989) An explanation for the indentation size effect in ceramics. Philos Mag Lett 59:281–288
27. Bull SJ (2003) On the origins and mechanisms of the indentation size effect. Zeitschrift fur Metallkunde 94:787–792
28. Chen J, Bull SJ (2006) On the relationship between plastic zone radius and residual depth during nanoindentation. Surf Coat Technol 201:4289–4293
29. Twigg PC, Riley FL, Roberts SG (2002) Nanoindentation investigation of micro-fracture wear mechanisms in polycrystalline alumina. J Mater Sci 37:845–853
30. Fujikani M, Setogarma D, Nagao S, Nowak R, Yamananka S (2007) Nanoindentation examination of yttria-stabilized zirconia (YSZ) crystal. J Alloy Compd 431:250–255
31. Williams DF (1981) Fundamental aspects of biocompatibility. CRC Press, Boca Raton
32. Elias CN, Lima JHC, Valiev R, Meyers MA (2008) Biomedical applications of titanium and its alloys. JOM 60:4649